

Modern Physics Letters B  
 Vol. 29, Nos. 35 & 36 (2015) 1530018 (27 pages)  
 © World Scientific Publishing Company  
 DOI: 10.1142/S0217984915300185



## Periodic oscillations of the forced Brusselator\*

J. A. C. Gallas

*Instituto de Altos Estudos da Paraíba,  
 Rua Infante Dom Henrique 100-1801, 58039-150 João Pessoa, Brazil  
 Departamento de Física, Universidade Federal da Paraíba,  
 58051-970 João Pessoa, Brazil  
 Max-Planck-Institut für Physik Komplexer Systeme, 01187 Dresden, Germany  
 Institute for Multiscale Simulation,  
 Friedrich-Alexander-Universität Erlangen-Nürnberg, 91052 Erlangen, Germany  
 jason.gallas@cbi.uni-erlangen.de*

Published 30 December 2015

We study the organization of stability phases in the control parameter space of a periodically driven Brusselator. Specifically, we report high-resolution stability diagrams classifying periodic phases in terms of the number of spikes per period of their regular oscillations. Such diagrams contain accumulations of periodic oscillations with an apparently unbounded growth in the number of their spikes. In addition to the entrainment horns, we investigate the organization of oscillations in the limit of small frequencies and amplitudes of the drive. We find this limit to be free from chaotic oscillations and to display an extended and regular tiling of periodic phases. The Brusselator contains also several features discovered recently in more complex scenarios like, e.g. in lasers and in biochemical reactions, and exhibits properties which are helpful in the generic classification of entrainment in driven systems. Our stability diagrams reveal snippets of how the full classification of oscillations might look like for a wide class of flows.

### 1. Introduction

This paper presents a systematic investigation of the global organization of oscillations, periodic or not, observed in several two-parameter sections of control parameter space of a periodically driven Brusselator. Of particular interest is to understand the unfolding of *periodic oscillations* and to describe what happens in the limit of low-frequencies and low-amplitudes of the external trigonometric drive.

Our objectives are twofold: First, to revisit and to extend certain aspects of earlier works. Thanks to more powerful computers, it is now possible to obtain high-resolution phase diagrams for the oscillator. Second, to show that this oscillator still harbors a plethora of unanticipated and interesting dynamical

\*This article will also appear in “80th Birthday of Professor Hao Bailin”, edited by Phua Kok Khoo and Ge Molin (World Scientific, 2016).

phenomena, particularly in the aforementioned low-frequency limit, where the system is dominated by periodicity and free from chaotic oscillations. We find the global organization of the complex oscillations to deviate in several aspects from what is currently known. Our basic tools of analysis are high-resolution phase diagrams obtained by using massive parallel high-performance computer clusters. We will also digress about some interesting open problems in driven oscillators. In the next Section, we sketch briefly the origin and some basic informations about the driven Brusselator, presenting then our results.

The existence of deterministic chaotic behaviors generated by oscillators of all sorts is now a well-established fact which occurs in virtually all field of science and is documented in innumerable books and surveys.<sup>1</sup> Despite the fact that the presence of the “randomly transitional phenomena”, discovered by Ueda<sup>2,3</sup> in 1961, or the “deterministic nonperiodic flows”, discovered by Lorenz in 1963, were first explicitly reported for flows, i.e. for systems of differential equations, most of the knowledge about chaotic behavior stems from investigations done on discrete-time nonlinear mappings. This fact is a simple consequence of the comparatively limited computational and graphical resources available in the early days. Furthermore, it is much simpler and more expeditious to iterate a discrete map than to integrate flows.

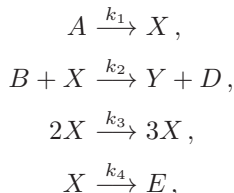
In flows, the existence of chaotic solutions has been traditionally illustrated either by projecting attractors into specific phase-space planes for selected parameter points, or by computing bifurcation diagrams along restricted parameter intervals. It is not uncommon to see recent papers reporting stability diagrams still consisting of a few simple curves delimiting the boundaries between phases characterized by the first few *periodic* oscillations, not the boundaries of periodic phases for “all” periods which lie well-beyond tame Hopf bifurcation borders, and not the boundaries of chaos. It is not yet standard practice to provide information concerning the actual inner structural organization of the chaotic phases, how abundant they are, if they contain internal subdivisions, accumulations, regularities, multistability, etc. In this context, an important open question is the quantification of the chaotic phases, of their boundaries and their evolution when parameters normally kept fixed are allowed to vary. These are questions that we wish to address here for the Brusselator. Together with the Belousov-Zhabotinsky reaction — reviewed in this volume by Field<sup>4</sup> — the Brusselator is among the most extensively studied flows.

## **2. Chemical Oscillations and the Brusselator**

### **2.1. *Origins of the Brusselator***

The origins of the oscillator known as Brusselator can be traced to a work in 1956 by Prigogine and Balescu<sup>5</sup> showing that undamped oscillations<sup>6–15</sup> are supported far from thermodynamic equilibrium in open chemical systems governed by nonlinear kinetic laws. This line of research was subsequently elaborated with the help of

abstract chemical models, one of them named “Brusselator” in 1973 by Tyson.<sup>16</sup> The name refers to a model studied in Brussels,<sup>7</sup> dealing with an autocatalytic process of the same type discussed much earlier, starting in 1910, by Lotka.<sup>11–15</sup> The scheme-I considered by Prigogine and Lefever is<sup>7,16</sup>



where  $A$  and  $B$  are input chemicals maintained at constant concentration,  $D$  and  $E$  are output chemicals, and  $X$  and  $Y$  are intermediates. The rate equations for the two intermediates are

$$\frac{dX}{dt} = k_1 A - k_2 B X + k_3 Y X^2 - k_4 X, \quad (1)$$

$$\frac{dY}{dt} = k_2 B X - k_3 Y X^2. \quad (2)$$

After proper rescaling these equations can be reduced to a system without superfluous parameters:<sup>16</sup>

$$\frac{dX}{dt} = A - B X + Y X^2 - k X, \quad (3)$$

$$\frac{dY}{dt} = B X - Y X^2. \quad (4)$$

where, for simplicity,  $k \equiv k_4$ . In the equations above we dropped a diffusion term which is not of interest here. For the standard linear stability analysis of the model above see, e.g. Section 2.2.5 in the book of Epstein and Pojman.<sup>17</sup>

As already mentioned, the (non-autonomous) Brusselator and the (autonomous) Belousov-Zhabotinsky reaction<sup>4</sup> are the two examples of (mathematical) flows that sparked almost simultaneously extensive studies of chaos in chemical reactions during the last four decades. However, after the coming-of-age of chaos, it is now becoming evident that the global organization of *periodic oscillations* presents many unsuspected surprises and that much still awaits to be discovered for them, particularly concerning the self-organization of oscillations in autonomous systems, free from the interference of external enslaving. In this context, we mention that periodic oscillations in chemistry already have an almost two-centuries long history, dating back at least to the beginnings of the 19th century as evidenced by the many experimental works collected and described in essentially forgotten books,<sup>9,10</sup> a history that needs to be better known.

Information about the dynamics of the Brusselator is collected in a 1977 book by Nicolis and Prigogine.<sup>6</sup> This book, however, is focused on the work of its authors and colleagues, not an overview of the field. While summarizing admirable things, connections with equally admirable earlier findings are not described. For

instance, Rosen<sup>18</sup> pointed out that “Irreversible thermodynamics, then, desires to treat dynamical properties of open systems by preserving the language historically developed to deal with equilibria in closed, isolated systems. This can be done, of course, but only through the introduction of a cumbersome and *ad hoc* formalism which, I believe, only serves to obscure underlying dynamical relationships. This formalism also serves to give an illusion of novelty to the dynamical study of open systems which actually dates back at least to Poincaré on the mathematical side, and in the sciences has been stressed by Bertalanffy [1932] and a host of others for forty years and more.” Rosen further adds: “. . . Historically, it was shown already by Rashevsky [1940] that, under appropriate conditions, reaction-diffusion systems could spontaneously generate and maintain spatially ordered states; he showed in particular how these mechanisms could generate polarities and gradients in initially homogeneous and isotropic cells (although Rashevsky was in fact the great pioneer in the study of reaction-diffusion systems in biology, his name is characteristically not mentioned in this connection anywhere in the book). The point of departure for the work of Prigogine and his school in self-organization was a paper of Turing [1952] which again showed, albeit in a much simpler context than Rashevsky, how spatial patterns could be established and maintained in autonomous reaction-diffusion systems. The present volume provides a systematic treatment of such systems, from the standpoint of irreversible thermodynamics.”

The work by Nicolis and Prigogine on the Brusselator<sup>6</sup> was also reviewed by Othmer,<sup>19</sup> who describes merits: “. . . there follows a sixty-six page analysis of some of the different types of bifurcations that can arise in the trimolecular reaction known as the Brusselator. Since this reaction scheme does not model any real chemical system, its main value lies in some of the behaviors of two-variable illustrating systems of nonlinear reaction-diffusion equations as simply as possible. However, there are equally simple models of real processes available (for instance, polynomial models of the glycolytic reactions mentioned in Chapter 8) that would serve better for this purpose in that some comparison between model predictions and experimental observations could be made. Nonetheless, the analysis of the Brusselator may prove useful to the neophyte in this area in that the often long and involved computations are spelled out in detail.”

Our motivation for studying the forced Brusselator is the desire to understand periodic and entrained oscillations. As it is known, depending on the amplitude and frequency of the external drive, the oscillations may emerge entrained either in a periodic, quasi-periodic, or chaotic mode. The original interest was in determining the extent in control parameter space of the various response regimes and understanding the transitions between them. Essentially, this is the basic problem to be solved for all sorts of nonlinear oscillators. It remains the outstanding problem in the field.

Another important motivation for studying the Brusselator is the fact that its undriven version is a limit-cycle system directly connected with much ongoing

research linked to Hilbert’s sixteenth problem, as described in several books.<sup>20–22</sup> Of special interest to us is to gather snippets concerning “simple” systems with cubic nonlinearities, the nonlinearities that we found recently to be frequently connected with wide-ranging organization of motions in the control space in several practical applications.<sup>23–33</sup>

## 2.2. Forced Brusselator: 1977–1982

Forcing was introduced in 1977 by Tomita, Kai, and Hikami.<sup>34</sup> They considered the equations

$$\frac{dX}{dt} = A - (B + 1)X + YX^2 + a \cos(\omega t), \quad (5)$$

$$\frac{dY}{dt} = BX - YX^2, \quad (6)$$

where  $a$  and  $\omega$  are the new freely tunable parameters controlling the external drive. In the absence of forcing, limit cycle behavior exists when<sup>16</sup>

$$B > A^2 + 1. \quad (7)$$

Under forcing, two coexisting stable oscillations were found<sup>34</sup> for the point  $(A, B, a, \omega) = (0.4, 1.2, 0.0018, 0.34)$ . Originally, the main concern was to determine the extension of the regions of entrainment and their stability. The limits of entrainment were estimated by using Floquet exponents and compared with results from numerical simulations. As a whole, Tomita, Kai, and Hikami<sup>34</sup> report finding a reasonable agreement between numerical and theoretical results, remarking however that despite the overall similarity between computed plots and theoretical estimations, “. . . an appreciable discrepancy is noted towards the low-frequency limit of entrainment.” This limit is discussed in detail below.

Subsequently, in a series of papers published during 1978–82, Tomita and Kai reported several additional results.<sup>35–39</sup> For instance, using a stroboscopic representation — see Chapter 16 of the book by Minorsky<sup>40</sup> — they obtained<sup>35</sup> the phase diagram shown in Fig. 1(a). In this diagram one sees a few resonance horns, a doubling cascade ending in chaos, indicated by the letter  $\chi$ . The hatched region was identified as a region of quasi-periodic oscillations. All these works focused on the dynamics of the  $\omega \times a$  control plane that is observed when fixing  $A = 0.4$  and  $B = 1.2$ .

The resonance horns for operating the Brusselator synchronously with the drive and with twice this period were reported by Knudsen *et al.*<sup>41</sup> Motivated by experimental studies for relatively large amplitudes of the forcing, these authors considered the structure of the resonance horns at intermediate and high amplitudes.

## 2.3. Frequency-amplitude diagram revisited

In this section, we reconsider the original frequency-amplitude diagram of by Tomita and Kai [Fig. 1(a)], presenting analogous results obtained in three distinct ways,

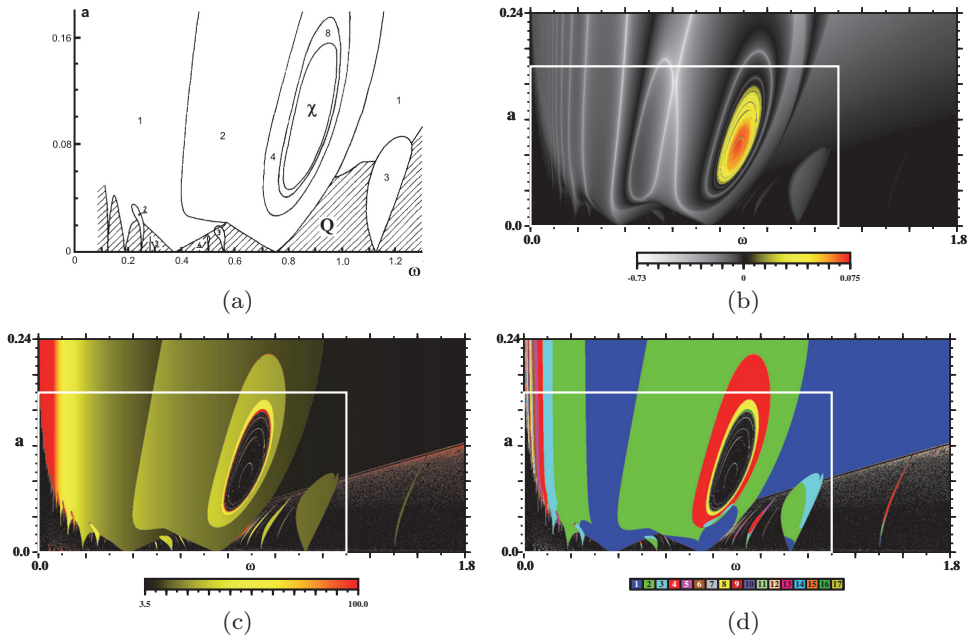


Fig. 1. (Color online) Four different frequency-amplitude stability diagrams recording entrainment regions for  $A = 0.4$  and  $B = 1.2$ . (a) Original stroboscopic Tomita–Kai representation.<sup>35,39</sup> (b) Lyapunov phase diagram, where colors indicate chaos (positive Lyapunov exponents). (c) Distribution of the period of the  $X$  oscillations. An identical plot is obtained for  $Y$ . Black marks non-periodic oscillations. (d) Number of spikes per period of the  $X$  oscillations. Black denotes chaos. Boxes in the last three panels delimit the parameter region in (a). Each bitmap displays the analysis of  $1200 \times 1200 = 1.44 \times 10^6$  distinct parameters.

presented in Figs. 1(b)–1(d). This will give us opportunity to introduce the stability diagrams to be used in the remainder of the paper. Such stability diagrams emphasize complementary aspects of the oscillations. Before discussing what the diagrams show, we explain how they were obtained.

Figures 1(b)–1(d) are bitmaps computed by dividing the parameter window into a mesh of  $N \times N$  equally spaced parameters, usually  $1200 \times 1200 = 1.44 \times 10^6$  points. Then, for each point of the mesh we computed three quantities: the Lyapunov spectrum, the period of the oscillations (if any), and the number of spikes contained in one period of the periodic oscillations of each component of the flow.

To this end, Eqs. (5)–(6) were integrated numerically using the standard fourth-order Runge-Kutta algorithm with fixed time-step  $h = 0.005$ . Integrations were always started from an arbitrarily chosen initial condition,  $(x, y) = (0.16, 1.16)$ , that was maintained fixed for all integrations. The first  $4 \times 10^5$  integration steps were disregarded as consisting the usual transient-time needed to approach the attractor. The subsequent  $80 \times 10^5$  time steps were used to compute the Lyapunov spectrum, Fig. 1(b). After computing the Lyapunov spectrum, integrations were continued for an additional  $40 \times 10^5$  time-steps, when we recorded up to 800 extrema (maxima

and minima) of the two variables of interest together with the instant when they occur. From this record, we determined repetitions of the maxima, obtaining for each parameter point the period (if any), plotted in Fig. 1(c), and the number of spikes per period. Figure 1(d) shows the spike count obtained from the variable  $X$ . A similar plot is obtained from  $Y$ .

We refer to stability diagrams like Fig. 1(d) to *isospike diagrams*,<sup>42–47</sup> i.e. diagrams where, for each variable of the oscillator, one may easily recognize from the colors both the size and the shape of oscillatory phases sharing the same number of spikes per period. A black dot is plotted when no periodicity was numerically detected. As indicated by the colorbar in Fig. 1(d) (and in similar figures below), a palette of 17 colors is used to represent the number of peaks (local maxima) per period. Patterns having more than 17 peaks are plotted by periodically recycling the 17 basic colors “modulo 17”: Multiples  $17 \times \ell$  of 17 are plotted with the color index corresponding to  $(18 - \ell) \bmod 17$ , namely  $34 \equiv 16$  for  $\ell = 2$ ,  $51 \equiv 15$  for  $\ell = 3$ ,  $68 \equiv 14$  for  $\ell = 4$ , etc.

The computation of these diagrams is numerically a quite demanding task that was performed using specially in-house developed FORTRAN software to generate each figure directly as Postscript bitmap output. To obtain the bitmaps we profited from the decisive help of up to 1536 processors of a SGI Altix cluster having a theoretical peak performance of 16 Tflops. While it is possible to observe period-doubling routes in the diagrams, most of the times what happens is just the addition of a new peak to the waveform (without a corresponding doubling the period). Note that the period is a quantity that evolves continuously when parameters are changed, while the number of peaks is “quantized”, namely a quantity that changes in discrete steps. The mechanism responsible for peak addition here is similar to the one observed in lasers and in other systems.<sup>29–31</sup> Eventually, after adding peaks one may reach a situation where the period roughly doubles a numerical value observed previously. But such coincidence occurs for a very specific parameter *value*, not for parameter *intervals*. The period may change not very much with parameters. Nevertheless, it is constantly changing and such changes are easy to detect numerically. The computation of the stability diagrams reported here is a standard calculation that we performed as described in detail previously, e.g., in Ref. 26 where efficient methods to deal both with numerical and experimental data are given. See also Refs. 23, 27, 28 and 33.

Comparing the three stability bitmaps in Fig. 1 one sees that the information conveyed by the Lyapunov diagram, Fig. 1(b), is quite limited: it merely reflects the dichotomic division of the control space into two regions, namely chaos and periodicity. The period diagram of Fig. 1(c) shows several additional boundaries, seen in Fig. 1(a) but which are not evident from the Lyapunov diagram. Although containing more structure, the continuous variation of the period scale does not inform what exactly is causing these boundaries, something that requires further investigation to be determined. In the window covered in Fig. 1(c), the maximum value of the period extends up to 3000, but for relatively limited subregions. Therefore, we

imposed an much smaller upper threshold of 100 for the period in order to avoid obtaining a solid black diagram. Next, comes the isoperiodic stability diagram in Fig. 1(d). It provides the same dichotomic separation between chaos and periodicity as the previous diagrams. However, in sharp contrast with them, Fig. 1(d) reveals a number of facts about the oscillations which are not discernible in the other diagrams. First, the several colors correspond here to oscillations having different number of spikes per period. Second, Fig. 1(d) shows (quantifies) the extension (volume) of the different multi-peaked phases of oscillation. Third, it allows one to discern the shape of the phase boundaries. Forth, it allows one to immediately recognize the *ordering* of neighboring phases. Fifth, it is easy to recognize the first few phases where oscillations undergo doubling of their number of spikes. Other phase complexities are also exposed. We reiterate, what is effectively doubling is the number of spikes, not the period, a quantity which varies continuously with parameters as may be recognized from Fig. 1(d).

In the remainder of the paper we will use isoperiodic diagrams because they convey much more information. Incidentally, recall that in his famous 1963 paper, Lorenz also used spikes of a chaotic oscillation to extract a return map with a cusp. Before proceeding, note that small localized differences among the high resolution panels can be detected. Such difference and certain discontinuities reflect regions of multistability, namely the presence of more than one attractor for a given parameter point. We made no attempt to tune initial conditions or parameters to avoid changes in basin of attraction. On the contrary, we find that such changes to be useful to indicate where multistability is more easily detectable.

Figure 1 contains a salient feature: a sort of “eye” of chaos, emerging as the accumulation limit of a doubling cascade. A natural question is to inquire about the extension of this eye of chaos around the Tomita–Kai parameter point  $(A, B) = (0.4, 1.2)$  and Fig. 2 provides an answer. The upper row shows stability diagrams obtained by varying  $A$ , while the bottom row illustrates similar plots obtained by varying  $B$ . From them one sees that the eye is less sensitive to  $A$  than to  $B$ . From the top row one recognizes a strong overlap arising from an entrained phase born near  $\omega \simeq 0.95$  when  $A = 0.37$ , a phase that moves to higher frequencies as  $A$  increases. The whole structure slides to the right. In contrast, from diagrams on the bottom row it seems that  $B = 1.2$  is very close to a transition threshold  $B_t$ : below  $B_t$  chaos is absent inside the window considered, while above it chaos is abundant. Furthermore, one also recognizes that the chaotic eye is quite localized along the  $B$  axis of the control space, in the sense that, at least in the interval considered, it exists just for a narrow  $B$  window. A curious feature on the bottom row is that, below the threshold  $B_t$ , one-peak oscillations subsist over wide frequency ranges independently of the amplitude of the drive, as long as the amplitude remains relatively small.

From Fig. 2 it is possible to recognize that, as the forcing amplitude  $a$  grows, there is an accumulation of many-peaked oscillations when  $\omega \rightarrow 0$ . This is indeed the case, a situation discussed in detail below.

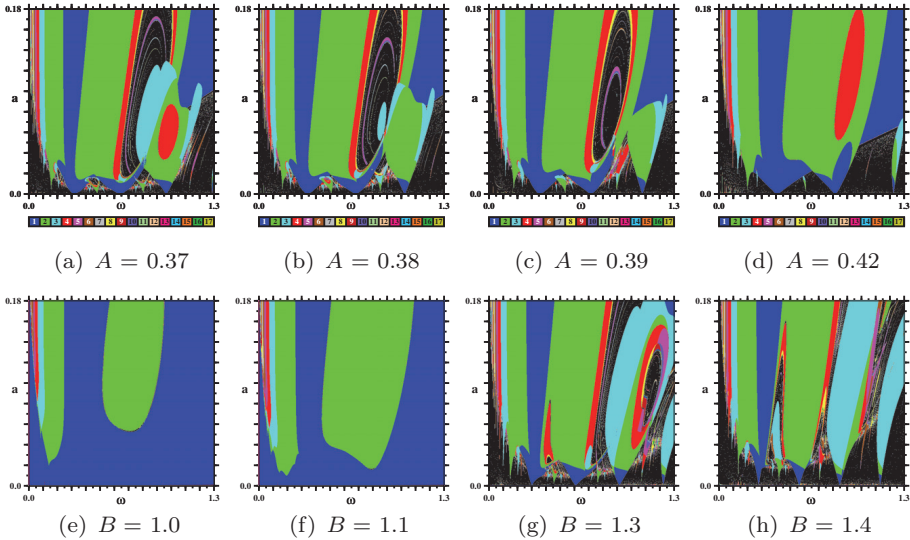
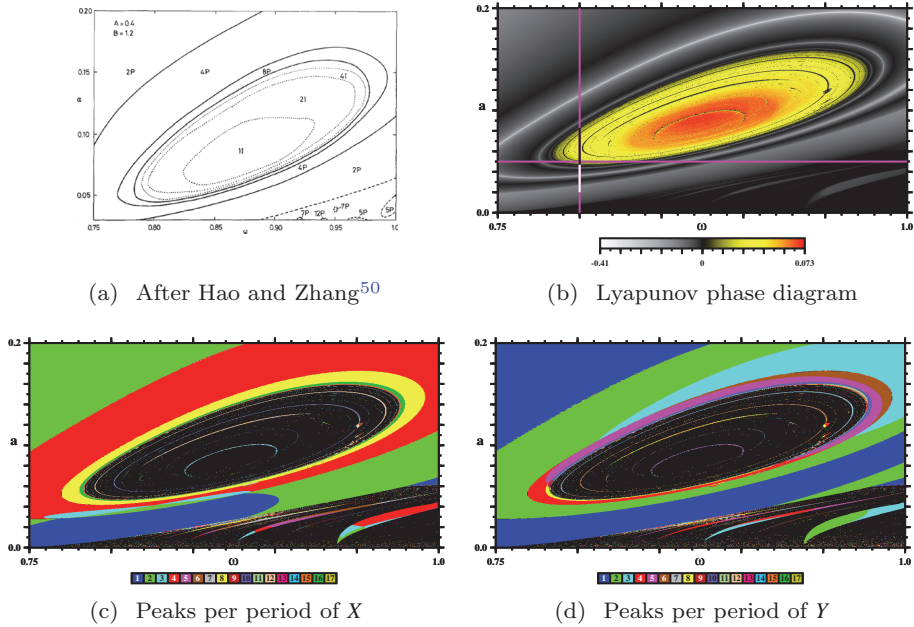


Fig. 2. (Color online) Frequency-amplitude diagrams: How dip is the hole with chaos around the point  $(A, B) = (0.4, 1.2)$ ? Stability diagrams illustrating entrainment and the distribution of spikes for slices of the control space. Top row: dependence on  $A$  for  $B = 1.2$ . Bottom row: dependence on  $B$  for  $A = 0.4$ . The color scale is the same for all panels.

#### 2.4. Forced Brusselator: 1982–1989

The driven Brusselator was also studied in a series of papers published in 1982–1989 by Hao, Zhang, and a coworker.<sup>48–52</sup> Their papers reported detailed phase diagrams obtained through a careful symbolic dynamics analysis. These works are reviewed at length in dedicated chapters in books.<sup>53–55</sup> Apart from supplementing information concerning the frequency-amplitude space reviewed above, Hao and Zhang<sup>50</sup> considered also two new parameter sections of the control space, namely the  $\omega \times A$  and  $\omega \times B$  planes. In a different spirit, Hao<sup>52</sup> reported phase diagrams drawn in an auxiliary  $\beta \times \gamma$  space, defined by the eigenvalues of  $\lambda_{\pm} = (\gamma \pm i\beta)\omega$  of the linearized problem. In this Section we reconsider briefly some aspects of these works, complementing them with details which can now be comfortably obtained thanks to modern computer clusters. We will only scratch the surface of their work, focusing on topics related to our interest. What follows is by no means a review of their extensive work.<sup>55</sup>

In 1982, Hao and Zhang<sup>48</sup> remarked that “sufficient high resolution” is a key to understanding the dynamics of oscillators, a perennial concern that remains valid today: “Direct period-doubling bifurcation sequences and inverse sequences of chaotic bands have been observed in a number of iterated maps. Many properties related to these bifurcations are shown or believed to be universal. There have been indications that nonlinear systems described by differential equations share such properties as well. To check this by numerical calculation we encounter the necessity of identifying the periodic and chaotic bands with sufficient high resolution. This is



details of the inner structure of the periodic phases. In these figures, colors reflect the number of spikes per period of  $X$  and  $Y$  respectively. As it is plain from the figures, the dichotomic separation into chaos and periodicity is the same in all diagrams. However, Figs. 3(c) and 3(d) allow one to additionally see that the subdivisions induced by the number of spikes depend strongly on the variable used to count them. As for Fig. 1, each isospike diagram on the bottom row of Fig. 3 displays a more informative classification than the Lyapunov diagram.

So far, all stability diagrams considered were obtained for  $(A, B) = (0.4, 1.2)$ . But Hao and Zhang<sup>50</sup> were also intrigued by what happens when one moves away from the parabola in Eq. (7), delimiting stationary states. They investigated two additional control windows, namely a window in the  $\omega \times A$  plane for  $(B, a) = (1.2, 0.05)$ , and a window in the  $\omega \times B$  plane for  $(A, a) = (0.4, 0.05)$ . They found these windows “look more complicated” than the frequency-amplitude window.

Figure 4 depicts what one finds on the  $\omega \times A$  plane. Figures 4(a) and 4(d) show relatively extended portions of this control plane, recorded by counting spikes

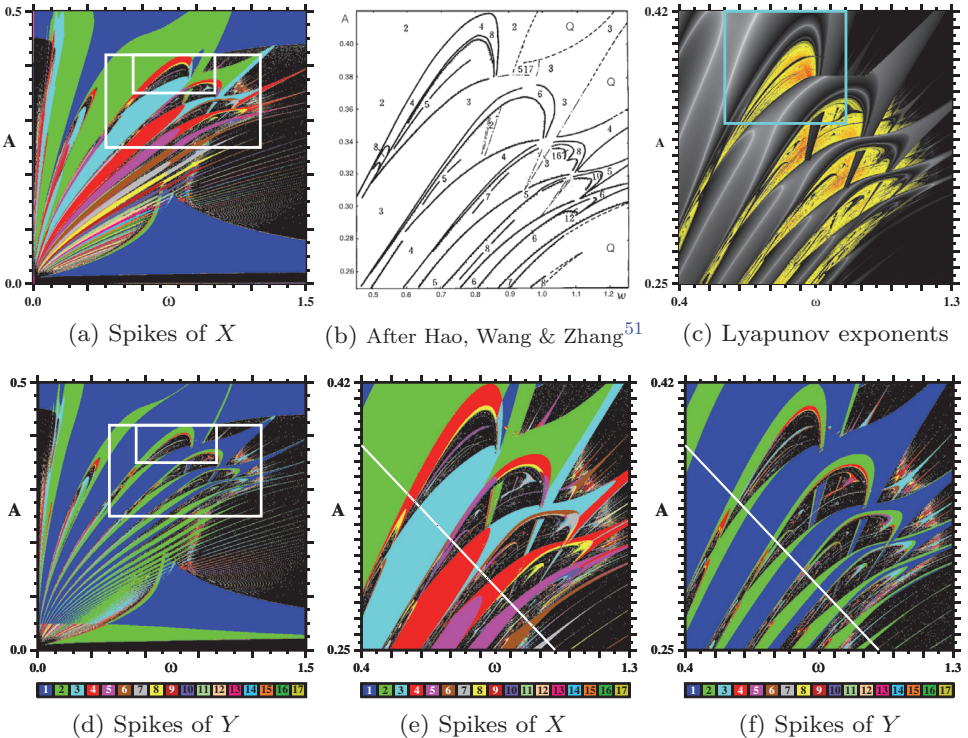


Fig. 4. (Color online) Sections of the  $\omega \times A$  control plane showing the location and details of a situation considered in panel (b), redrawn after Hao, Wang & Zhang.<sup>51</sup> The slanted lines in (e) and (f) are discussed in connection with the point listed in Table 1. Here  $a = 0.05$ ,  $B = 1.2$ . Note the greater spike diversity of  $X$ . Each bitmap displays the analysis of  $1200 \times 1200$  parameter points.

of  $X$  and  $Y$ , respectively. They contain a pair of boxes indicating the windows considered by Hao and Zhang. The content of the smaller box is sketched in Fig. 9 of the paper.<sup>50</sup> A more detailed view of the larger box, obtained from a stroboscopic map, was given in 1983 as Fig. 1 of Hao, Wang, and Zhang<sup>51</sup> and as Fig. 1 of Hao's review.<sup>56</sup> This window is reproduced here in Fig. 4(b). For this same window, we present three additional stability diagrams: the standard Lyapunov diagram [Fig. 4(c)], and a pair of diagrams, Figures 4(e) and 4(f), obtained by counting spikes of  $X$  and  $Y$ , respectively. These diagrams illustrate that the basic features are well represented in Fig. 4(b). It is also possible to recognize a quite complicated alternation of colors visible in the myriad of smaller phases in Figs. 4(e) and 4(f) as well as in certain regions in Figs. 4(a) and 4(d). These complex organizations of stability phases were recently observed and described in rather different contexts, namely in series of nested arithmetic progressions of oscillatory phases arising in a simple enzyme reaction model introduced by Olsen,<sup>24</sup> and as nonchaos-mediated mixed-mode oscillations in a state-of-the-art model of the same enzyme reaction.<sup>25</sup>

In Figs. 4(e) and 4(f) one sees the slanted white line  $A = 0.46 - 0.2\omega$ . This is a line considered by Hao and Zhang,<sup>50</sup> in Table 5.20, page 300, of Hao,<sup>53</sup> and in Table 6.4, page 327, by Hao and Zheng.<sup>54</sup> Along this line, they considered specific points  $(\omega, A)$  reproduced here in Table 1. For these values of  $\omega$  are characterized by specific symbolic codings. The table contain  $\omega$  values corresponding to the symbolic codings of all periods up to 7. Since there is no connection between symbolic sequences and stability, the  $\omega$  intervals defined in Table 1 do not correspond to the stability intervals observed along the slanted lines. For each  $\omega$ , Table 1 collects some orbital indicators: the number of spikes per period of  $X$  and  $Y$ , and the value of the period  $T$ . From this table one sees that it is possible to recognize that the several indicators listed do not agree uniformly along the slanted line.

Figure 5 depicts stability phases of oscillations found for an extended range of the  $\omega \times B$  control plane, as recorded by counting spikes of  $X$ . The dominant blue color of the series of parallel stripes represent 1-peaked oscillations while black denotes chaos. Figure 5(a) shows the region where the dynamics changes more. The box in it is shown enlarged in Fig. 5(b), which contains four additional boxes, shown magnified on the bottom row. When moving towards smaller values of  $\omega$ , the blue stripes are separated more and more by domains where very complex alternations of periodic phases can be seen [Figs. 5(c)–5(f)]. On the scale of Fig. 5(a) such regions seem to display some mild similarity but, in fact, every stripe has its own characteristic inner organization, as illustrated on the bottom row.

Figures 5(c)–5(f) display quite different organization of the oscillatory phases. In fact, it is quite difficult to describe them by other means than representing them graphically. Here, colors are very helpful to distinguish their exquisite organization. Recall that these figures represent cuts obtained for the specific values of  $A$  and  $a$  mentioned in the figure caption. Changes of these values implies changing the distribution of the phases plotted. Therefore, a proper understanding and description of these phases would require investigating how they evolve when the

Table 1. Comparison of distinct characterizations of the oscillations for points along the line  $A = 0.46 - 0.2\omega$  [white line in Fig. 4(e)], studied with symbolic dynamics and collected in Table 5.20 of Ref. 53 (see also Hao and Zheng<sup>54</sup>). “Hao’s  $p$ ” refers to the period listed in Table 5.20. The distinct indicators do not agree uniformly for all values of  $\omega$ .

#	Hao’s $p$	Pic- $x$	Pic- $y$	$\omega$	$T$	$\omega T/(2\pi)$
1	2	2	1	0.54400	23.09950	1.9999614
2	4	2	1	0.55500	22.64250	2.0000345
	4	4	3	0.57770	43.50500	4.0000155
3	6	6	4	0.58249	64.72100	6.0000356
	6	—	—	0.58251	chaos	chaos
4	5	5	3	0.58450	53.74850	5.0000114
	5	5	3	0.58480	53.72050	4.9999716
5	3	3	2	0.59470	31.69550	2.9999615
	3	3	1	0.65400	28.82200	3.0000051
6	6	3	1	0.65450	28.80000	3.0000070
	6	5	3	0.70250	53.66450	6.0000317
7	5	5	2	0.70680	44.44800	4.9999872
	5	5	3	0.71150	44.15450	5.0000000
8	6	6	3	0.71800	52.50600	6.0000312
	6	6	3	0.71850	52.46900	5.9999785
9	4	4	2	0.73250	34.31100	4.0000105
	4	3	1	0.79200	31.73300	3.9999673
10	7	6	2	0.80350	54.73850	7.0000139
	7	6	3	0.80560	54.59550	6.9999742
11	—	—	—	forbidden	forbidden	forbidden
12	7	6	4	0.81940	53.67500	6.9998405
13	5	—	—	0.82590	chaos	chaos
	5	4	1	0.86750	36.21500	5.0000933
14	6	5	2	0.90150	41.81750	5.9998988
	6	5	1	0.92300	40.84250	5.9997638
15	7	6	2	0.95900	45.86500	7.0003562
	7	6	2	0.97400	45.15750	7.0001763

additional parameters are tuned. This is something that demands a huge investment of computer time and will not be attempted here.

An interesting open question is to try to understand what sort of mechanisms generate 1-spike stripes over relatively wide regions and then, with a certain regularity, produce very complex alternation of stable oscillations with spikes that grow in number with apparently no upper bound. This growth may be easily corroborated by additional enlargements of smaller and smaller parameter regions (not shown here). Next, if instead of  $X$  one uses  $Y$  to count the spikes, then the same overall dichotomic distribution of periodicity and chaos is obtained but the alternation of the phases is by far less complex than in Fig. 5, similarly to what happens between Figs. 4(a) and 4(d). Why this is so is not understood yet. Another interesting question related to these diagrams is to understand what is behind the several parameter accumulations discernible in them, and why they occur in very specific regions of the diagrams.

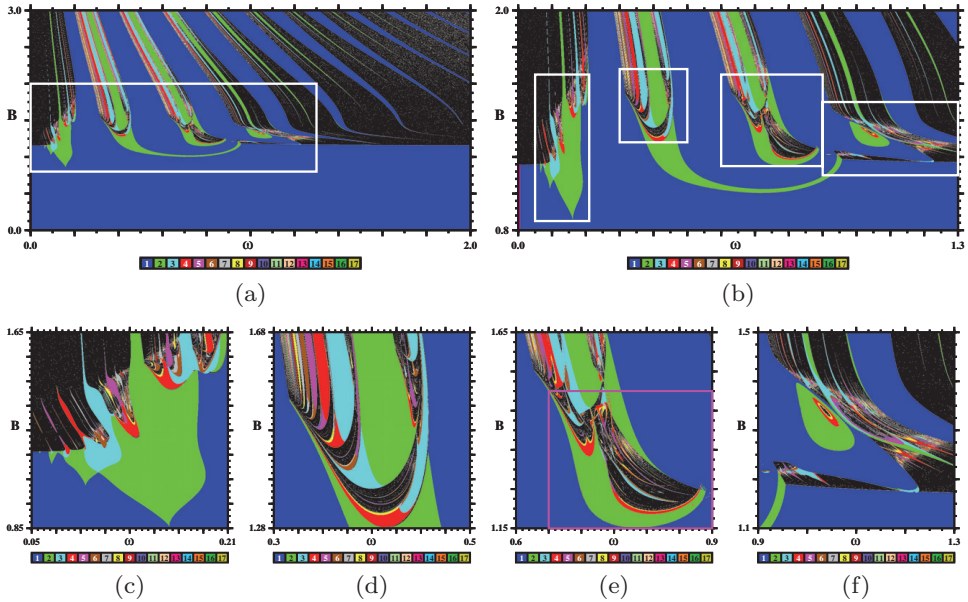


Fig. 5. (Color online) Successive enlargements illustrating the complex distribution of oscillatory phases recorded from the spikes of  $X$  on the  $\omega \times B$  plane. The box seen in (e) marks a region considered earlier by Hao and Zhang.<sup>50</sup> Here  $A = 0.40$ ,  $a = 0.05$ . Each bitmap displays the analysis of  $1200 \times 1200$  parameter points.

### 3. Low-Frequency Limit: Mosaic Tilings

Careful examination of the three distinct parameter sections discussed so far reveals several regions where the number of spikes varies considerably. One such region is the  $\omega \rightarrow 0$  limit in the frequency-amplitude diagrams in Fig. 1. As far as we know, these complex accumulations of oscillations were not yet considered in the literature. The purpose of this Section is to describe them qualitatively in some detail.

Figure 6 illustrates the complex alternation of stability phases typically found in the  $\omega \rightarrow 0$  limit. In this limit, the stability diagram turns into regular mosaics of phases which organize themselves differently along certain specific regions. For instance the regular organization seen on the left of the upper part of Fig. 6 seems to be interrupted on the boundary formed by domains like the ones labelled  $B, E, g_3$  and the domains labelled  $A, D, g_2$ . These latter domains preserve the systematics seen on the domains above them but the relative *size* of the domains changes significantly when crossing the aforementioned boundary. Similarly, there is another discontinuity when passing from  $G, J, M$  etc to  $H, I, L$  etc. Additional discontinuities exist but are less evident. They would require enlargements to be seen more easily.

Conspicuous in Fig. 6 is the absence of chaotic phases for low frequencies. In this region, the number of spikes per period grows steadily by one when moving towards the left of the diagram. The rapid alternation of the colors indicates that

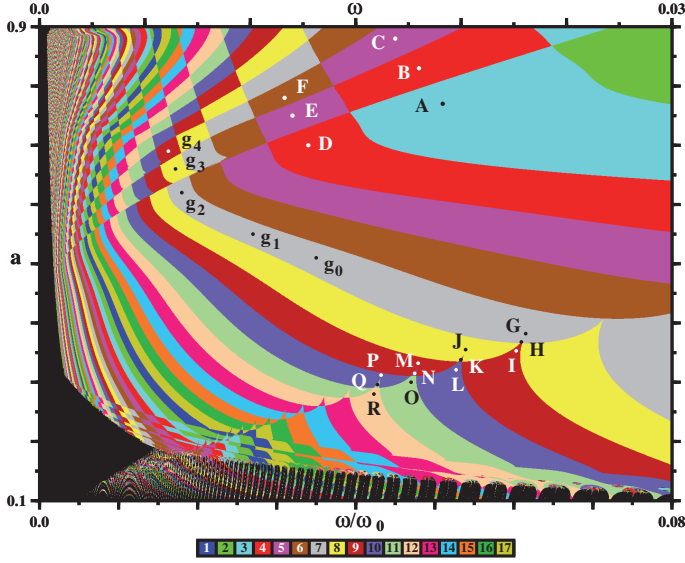


Fig. 6. (Color online) Mosaic tiling observed in the limit of low-frequency and small amplitudes, recorded from the spikes of  $X$ . Here  $(A, B) = (0.4, 1.2)$ . In the absence of the external drive, the angular frequency the oscillator is  $\omega_0 = 0.375$ .

Table 2. Characteristics of the oscillations for the points marked in Fig. 6, when  $(A, B) = (0.4, 1.2)$ . Coordinates  $(\omega, a)$ , the period  $T$  of the oscillations, and the number of peaks contained in one period of  $X$ . In the absence of the drive,  $\omega_0 = 0.375$ .

	$\omega/\omega_0$	$a$	Period	# peaks		$\omega/\omega_0$	$a$	Period	# peaks
A	0.051	0.77	328.535	3	J	0.0539	0.355	310.855	8
B	0.048	0.83	349.065	4	K	0.0533	0.338	314.355	9
C	0.045	0.88	372.34	5	L	0.0527	0.316	317.935	10
D	0.034	0.7	492.8	4	M	0.0479	0.332	349.795	9
E	0.032	0.75	523.6	5	N	0.04745	0.315	353.11	10
F	0.031	0.78	540.49	6	O	0.047	0.3	356.495	11
G	0.0615	0.382	272.44	7	P	0.04320	0.312	387.85	10
H	0.06095	0.368	274.9	8	Q	0.04275	0.296	391.935	11
I	0.0603	0.353	277.86	9	R	0.0423	0.28	396.105	12
$g_0$	0.035	0.51	478.72	7	$g_2$	0.018	0.62	930.845	7
$g_1$	0.027	0.55	620.565	7	$g_3$	0.0172	0.66	974.14	8
					$g_4$	0.0163	0.69	1027.925	9

the number of spikes per period grows very fast towards  $\omega = 0$ . Rather than chaos, the black region near  $\omega = 0$  seems to reflect difficulties of the algorithm to separate the series of very small amplitude peaks which proliferate more and more in the solutions. By tuning the integrator and using longer transients we were able to complement the diagram more and more near  $\omega = 0$ , giving us the impression that, in fact, there is no upper bound on the number of peaks, just on the amount of time and effort that one is willing to spend in order to complete the diagram in this region. As may be recognized from the figure, the double limit  $\omega, a \rightarrow 0$  is even

trickier and deserves further study. Be it as it may, in the present paper we just wish to address what is causing the large mosaics easily discernible in the figure, not their possible existence down to  $\omega \rightarrow 0$ .

To investigate more closely the phases with distinct number of spikes underlying the tiling in Fig. 6, we computed the temporal evolution for a number of representative points, indicated by the several labels in the figure. Their coordinates, period and number of peaks are listed in Table 2.

Figure 7 displays the temporal evolution for the triplet of points labelled  $A, B, C$  and  $D, E, F$  in Fig. 6. The number of spikes increases in two distinct parts of the oscillatory signal: inside the boxes in each panel, and around the minimum value of the oscillations. Along the vertical columns in Fig. 7, the number of spikes remains constant inside the boxes, namely they are constant for the triplets  $A, B, C$  and  $D, E, F$ , etc. In contrast, the total number of spikes increases downwards by one as the amplitude  $a$  increases. This allow one to grasp what sort of mechanism is acting to produce the tiling seen on the leftmost upper corner of Fig. 7: a proliferation of spikes near the minimum.

Next, Fig. 8 presents a detailed view of the spikes unfolding near the cusp-like patterns marked in Fig. 6 by triplets of points labelled  $G, H, I, J, K, L, M, N, O$ , etc. In every triplet, the middle point, namely, points  $H, K, N, Q$  where chosen very near to the cuspidal point. In Fig. 8, red dots denote local maxima of  $X$ ,  $z_\ell$  refer to successive magnifications of the box seen on the bottom of each panel, and the arrows point to the birth of a new spike. From the sequence  $z_\ell$  of magnifications we may identify a sort of “spike gun” inside box  $z_4$  which is shooting spikes to left, one by one.

What happens when moving across one of the many elongated phases stretching roughly diagonally in Fig. 6? An answer is given in Fig. 9, where we represent the temporal evolution of  $X$  for the six points  $G, g_0, g_1, \dots, g_4$  marked in Fig. 6. From this figure it is clear from the outset that the four points  $G, g_0, g_1, g_2$  must all have seven spikes, with additional spikes emerging for  $g_3$  and  $g_4$ . From Fig. 9 one sees that two major changes happen when moving from  $G$  to  $g_2$ : (i) The amplitude of the oscillations is greatly reduced when the amplitude  $a$  of the external drive increases, and (ii) the period of the oscillations increases considerably with  $a$ . The spike-adding mechanism acting when moving from phases  $g_2 \rightarrow g_3$  and from  $g_3 \rightarrow g_4$  is similar to the one acting when moving from  $D \rightarrow E \rightarrow F$  and from  $A \rightarrow B \rightarrow C$ , already described in Fig. 7. Along the upper phase boundaries of Fig. 6, new spikes get added one by one near the minima of the oscillatory signal. From  $g_2$  to  $g_3$  a negative spike of large intensity appears. It is the first of a train of similar spikes but with smaller and smaller intensity as  $a$  increases and  $\omega \rightarrow 0$ .

Figures 7–9 allow one to understand the nature of the spike-adding mechanism at work to form the regular tiling observed at low frequencies. In this interesting region, the relatively slowly varying oscillations acquire localized trains of spikes that get more and more low-amplitude spikes as the amplitude  $a$  of the drive grows, and as its frequency tends to zero. As mentioned before, while it is numerically

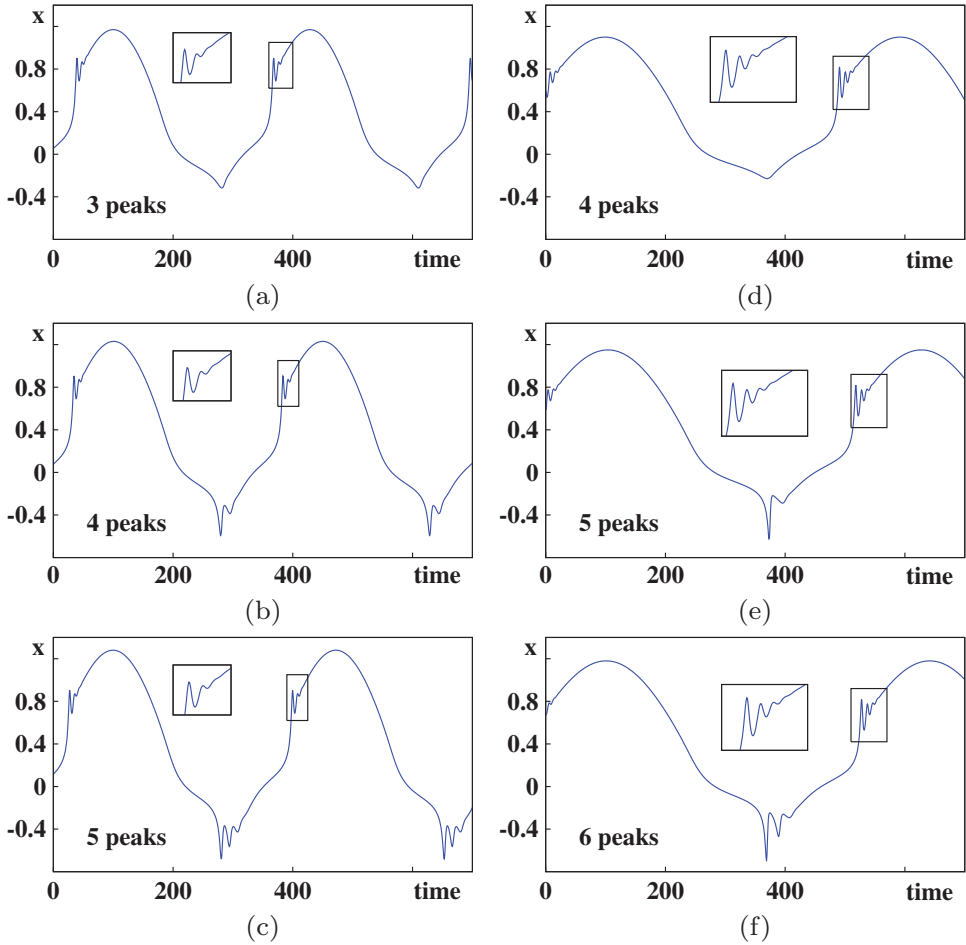


Fig. 7. New spikes emerge one by one, near the minimum of  $X$ , when the amplitude  $a$  of the drive increases vertically along the triplets of points  $a, b, c$  and  $d, e, f$ , marked in Fig. 6. The insets show details of the number of peaks in the upper part of the oscillations. The number of spikes in the inset remains constant along vertical sequences.

demanding to repeatedly tune the integrator and initial conditions to detect large number of spikes with tiny differences in their amplitudes, the general trend seems clear and unlikely to bring additional surprises in this range. Such localized trains of pulses with an unbounded number of spikes induce nice tilings in phase diagrams like the one in Fig. 6. Before moving on, we mention that the stability diagram corresponding to Fig. 6 obtained by counting spikes of  $Y$  (instead of  $X$ , as in this figure) has a rather similar structure but with an additional change of phases occurring along the line  $a = 0.425$ , and a few other details whose discussion we now postpone.

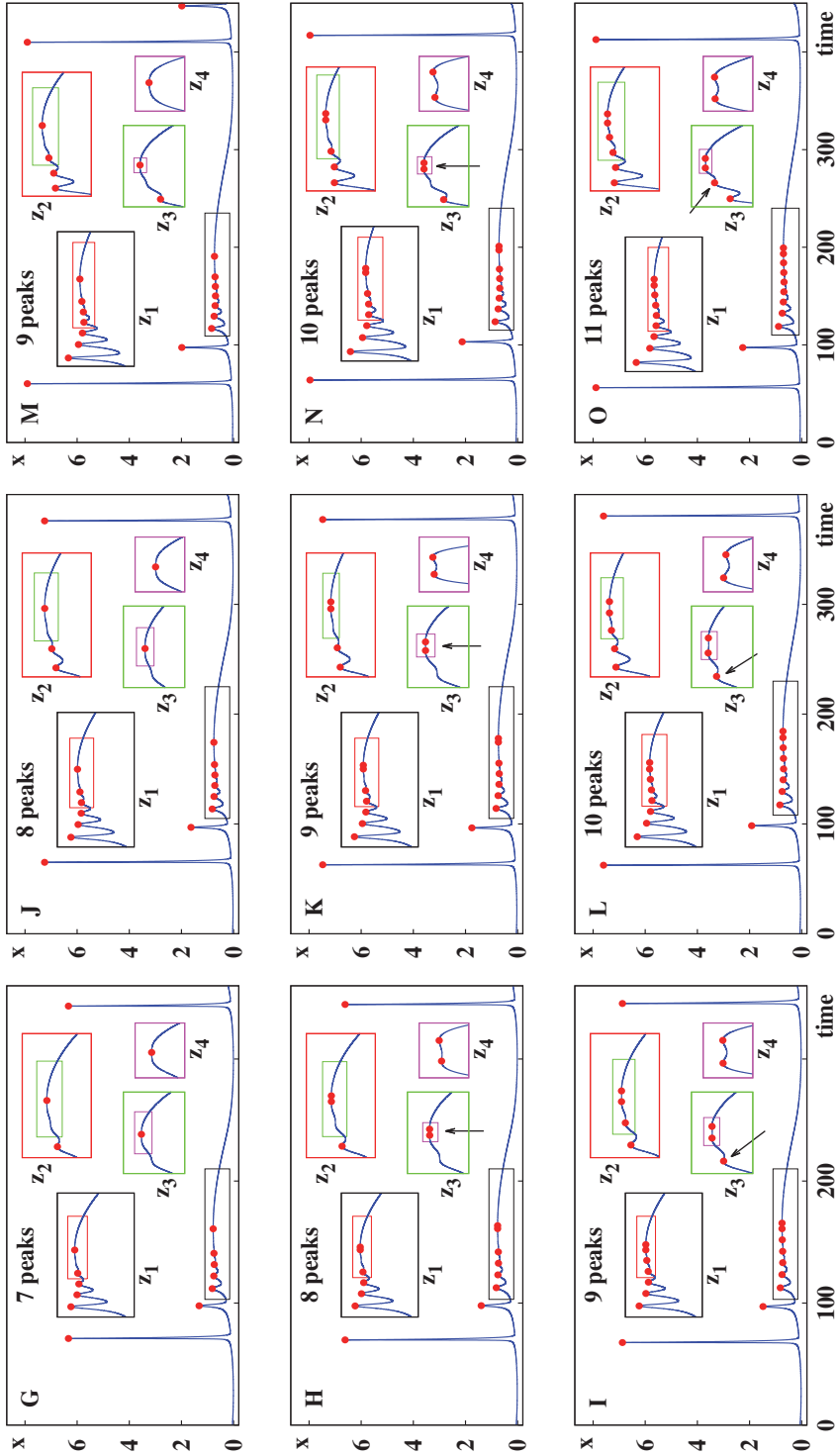


Fig. 8. (Color online) Details of the spike generating mechanism acting near the cusp-like patterns close to the triplets of points  $G, H, I$  and  $J, K, L$ , marked in Fig. 6. Red dots denote local maxima of  $X$ ,  $z_\ell$  refer to successive magnifications of the box on the bottom, and arrows indicate birth of a new spike. Inside box  $z_4$ , new spikes are “fired” to the left, one by one.

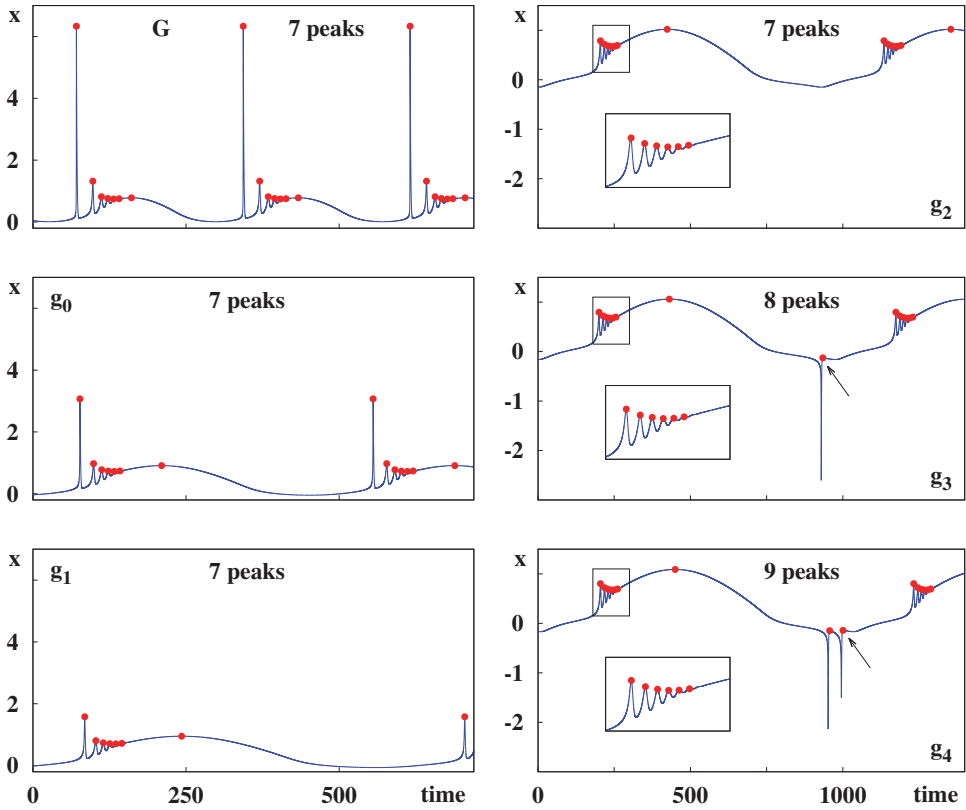


Fig. 9. (Color online) Evolution of the waveform of  $x$  along the 7 spikes' strip and the genesis of new spikes which form a mosaic-like pattern. The red dots marked maxima of  $x$  and the arrows locate new emerging peaks. Coordinates of the points  $G, g_0, g_1, \dots, g_4$  and the period of  $x$  are given in Table 2.

#### 4. Changes of Plane $B \times A$ Under Forcing

As mentioned above, an important motivation to consider modifications of the  $B \times A$  control plane of the Brusselator is its connection with Hilbert's sixteenth problem and our interest in studying oscillators with cubic nonlinearities. In the absence of drive, the Brusselator is a two-dimensional system and the Poincaré-Bendixson theorem precludes the onset of chaos. Thus, only limit cycles may be present and the question is counting their quantity as a function of  $A$  and  $B$  and determining the size of the individual basins of attractions. In this context, an interesting question is to find out the structural modifications of the oscillatory phases and their number when in presence of an external drive of small amplitude. As far as we known, the control plane  $B \times A$  was not yet considered for the driven oscillator.

Figure 10 illustrate that intricate alternation of phases typically observed on the  $B \times A$  plane when the amplitude  $a$  of the external drive grows for a given frequency, here  $\omega \equiv 1$ . In sharp contrast with the very small number of spikes detected in the

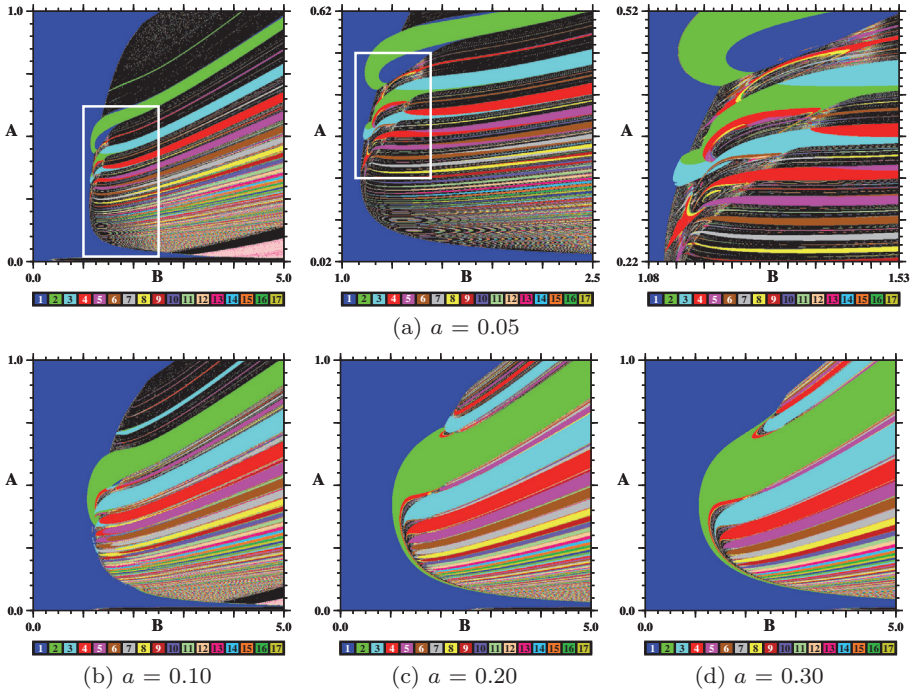


Fig. 10. (Color online) Impact of the growing amplitude  $a$  of the external drive on the  $B \times A$  plane when  $\omega = 1$ . Top row: successive magnifications of the regions inside the box. Bottom row: overall compression induced by larger amplitudes  $a$ . Each bitmap displays the analysis of  $1200 \times 1200$  parameter points.

limit cycles typically present in polynomial systems,<sup>20–22</sup> even the relatively small amplitude  $a = 0.05$  is enough to induce a large number of stable oscillations with an apparently unbounded number of spikes. This is illustrated by the three stability diagrams on the top row of Fig. 10. As observed previously for the other control parameter planes, the plane  $B \times A$  also displays specific “directions”, or paths, where large number of spikes accumulate. It also contains large phases of chaos “bridges” similar to the ones reported recently in a model of an enzyme reaction.<sup>24</sup>

The three panels on the bottom row of Fig. 10 show that the overall structure of the stability diagrams are not strongly affected when  $a$  further increases. The major change is a sort of “pinching effect” along the vertical coordinate, with the phase ordering remaining isomorphic but with chaotic phases significantly reduced as  $a$  grows. Of course, this pinching has nothing to do with the homonymous effect in plasma physics. The  $B \times A$  plane will be considered with more detail elsewhere.

## 5. Reminiscences

This paper is dedicated to Prof. Hao Bailin, on the occasion of his 80th birthday. In this special Section we collect some personal reminiscences related with his many publications in nonlinear dynamics.

While collecting information for this paper the author had the privilege of exchanging emails with Dr. Tohru Kai and Prof. Hao Bailin, concerning early work on the driven Brusselator. One email from Prof. Hao Bailin is so rich on informations about his original work on the Brusselator, about his motivations for studying it, and delightfully intertwined with personal remarks that, with the kind permission of its author, it is reproduced here *in toto*.

### **5.1. *Unsuspected impact of Hao Bailin writings***

Our motivation for selecting the driven Brusselator is that it was also the object of a contribution by Prof. Hao Bailin, presented in 1987 in a volume dedicated to Prof. Kazuhisa Tomita, on the occasion of his retirement from the Kyoto University.<sup>56</sup> So, it is with great pleasure that I outlined some findings of recent and current studies of the forced Brusselator, offered as a contribution in the *Festschrift* honoring Professor Hao Bailin. His publications in nonlinear dynamics include several papers on the problem of describing and interpreting the complexities associated with the general field of *deterministic chaos*. The many contributions of Hao Bailin and his wife Zhang Shuyu also include influential books and monographs on chaotic dynamics where much information and valuable references to the literature can be found.

Such books were extremely useful in the early days of my studies because, living and working very far away from big scientific centers, access to information was very limited. Nowadays, the younger generation can hardly imagine how difficult it was in the pre-historic days, i.e. before the internet, to obtain and to exchange information. Back then, information was essentially limited to printed journals and books. Thus, to create and maintain local libraries was very critical. Every year, our library needed to apply for funds to pay journal subscriptions, ask for all pro-forma invoices, go after requests lost in the “snail-mail”, send out applications and justifications to the central government and await for the inescapable cuts and the approval. After all that, because of strict restrictions for spending hard currencies, the library needed to start lengthy bureaucratic procedures to pay several different publishers abroad, each one requiring separate banking transactions and paper work. So, it was not uncommon to receive only by the end of every year a few precious boxes containing *all together the journal issues of the last 11–12 months*. And then to restart the whole procedure anew!

One of the best physics libraries in South America is located in Porto Alegre, Brazil. It owes much to the diligent work of a dedicated librarian, Zuleika Berto, who during several decades, even after her retirement, zealously collected materials, organized them, and trained a host of other librarians to help maintain the collection. In this library, it is still possible to check today journal covers for rubber stamps marking their clustered abrupt arrivals, not scattered along the year as one would normally expect. That such dates are well preserved today is of course a “benefit” of never having funds to bind the journals (thereby removing their

covers). Curiously, when photocopies were still popular, we could obtain them much easier and in much readable form from our not binded journals than abroad, from large and heavy bounded volumes. All this gives a glimpse into the importance of being then able to ask colleagues traveling abroad to smuggle into the country the books and monographs of Hao Bailin and Zhang Shuyu: apart from their valuable scientific contents, the references that they diligently gathered allowed us to write the then common post-cards to colleagues abroad, hoping to obtain in return, by quite slow mail, copies of their new and old publications. Dear Prof. Hao Bailin, thank you very much for this non-orthodox help provided by your works and for all the inspiration from your many contributions!!

## **5.2. *Reminiscences of Hao Bailin***

I was born on 26 June 1934 in Beijing. A few months before my birth my father Kingsheng Hao went to Berlin to do his PhD in botany and forestry (eventually he got two degrees and used to call himself Dr. Hao in the German way). Therefore, I was given the name Bailin. Bailin means cypress forestry and it is also the Chinese transcription of Berlin, the capital of Germany.

Shuyu Zhang was born a few months earlier than me in a town in province Jiangsu, on the northern bank of the mouth of the great Yangtze River. We did not know each other until the second half of 1953. In 1953 we graduated from different high schools in Beijing and took part in the nation-wide entrance examination for higher education. Apparently, we both got good scores and were accepted not by any university but by a preparatory class at Beijing Institute of Russian Language to be sent by the government to USSR. Although I was dreaming to become a physicist and Zhang a chemist, the authorities did not care about our personal wish.

In the fall of 1954, together with 14 fellow students, we were sent to Kharkov Institute of Engineering Economics in the now Ukranian city Kharkov. I was assigned a major “Organization and Economics of Coal Mines”, and Zhang a similar major for metallurgical industry. In September 1956 I managed to transfer to the Department of Physics and Mathematics of Kharkov State University. (Well, I skip the lengthy and painful story of how this was done.) I spent 3 years to complete the 5-year program of physics. In 1959 with Shuyu we got back to Beijing in the same trans-Siberian train. We got married soon after.

I was sent to USSR again in the fall of 1961 to do graduate study. Being already a physicist I had a little more freedom. I registered at Moscow State University and started working with Lev Davidovich Landau at the Institute of Physical Problems, USSR Academy of Sciences. Perhaps you have heard about the Landau Barrier (a set of 10 examinations). I passed it in 10 months, but, unfortunately, Landau got injured in a car accident in January 1962 just after I successfully took the first math exam with him. Landau never recovered and died in 1968. I continued to work with Alex Alexievich Abrikosov, the 2003 laureate of Nobel Prize in physics. I did not

finish the graduate study as the relation between the two countries went down and I returned to China the summer of 1963. I worked in the Institute of Physics, CAS, from 1959 to 1978. I took part in the establishment of the Institute of Theoretical Physics, CAS, in 1978 and worked there from 1978 to 2005. I worked in nonlinear dynamics from 1980 to 1998, and in theoretical life sciences from 1997 to the present time. In 2005 I moved to Fudan University in Shanghai and established a T-Life Research Center there (T-Life means Theoretical Life Science).

My wife Shuyu worked in the Planning Department of the Ministry of Metallurgy since 1959. Her department was disbanded during the “Cultural Revolution” (1966–1976) and she was sent to countryside to be re-educated by the farmers. In 1972, upon return to Beijing, she was assigned a job in another technical department. At my suggestion she started working in computer programming on China-made transistor-based computers. For a few years she worked on LISP language and algebraic manipulation software. She retired in 1993 as a Senior Software engineer at the Institute of Physics, CAS. That was why and how she became my collaborator.

*Details about Hao-Zhang papers:* Before answering your questions one by one, I think the following recollection may help to clarify some of the points you raised. In 1978, being a member of a delegation of CAS to Japan, I had a chance to discuss with Prof. Tomita in his office at Kyoto University. He showed some results on chaotic orbits in the periodically forced Brusselator. At that time I had almost no idea about chaos and soon forgot it. In 1981 I was invited by Ilya Prigogine to the Free University of Brussels for a half-year visit. Prof. Hermann Haken, whom I met in 1977 during a visit to Stuttgart, took the chance to invite me to attend one of his early synergetics symposiums held at Schloss Elmau. The theme of the meeting was “Chaos and Order in Nature”. Together with Shuyu we spent a week on the snow-covered slope of German Alps. Most participants talked about chaos, but I reported on order, namely, a closed-form approximation for the three-dimensional Ising model (it was published in the symposium volume edited by Haken, Springer-Verlag).

On our way back to Brussels we discussed the news heard at Schloss Elmau and decided to look at chaos in differential equations. A simple question was whether there exist the same Feigenbaum constants in period-doublings in ODEs. At this time I recollected what Tomita told me and suggested Shuyu to look at the forced Brusselator. I already know that there is no chaos in autonomous ODEs of two variables such as the simplified tri-molecule model for the BZ reaction, called Brusselator by Tyson. Anyway, since we were visiting Brussels it was reasonable to pick up an ODE related to Brussels.

At that time the Computing Center of the Free University of Brussels had just updated their mainframe to CDC Cyber2000. Shuyu soon realized that most of the users had not got accustomed to the new computing power yet. The system often ran idle during nights and weekends, so she started submitting a great number of jobs, while I was working on other problems. She even got protest from other

colleagues that the user queue was some times filled with her jobs only. Then she studied the JCL (Job Control Language) of the Cyber computer and invented a way to chain-up her jobs so only no more 4 jobs were visible in the queue at any time. I was occupied by my own non-chaotic problems until one day Shuyu showed me the periodic windows she discovered along a straight line in the parameter space. I should admit that it was Shuyu who forced me eventually to get into symbolic dynamics. The SSS (Subharmonic Stroboscopic Sampling) method, the slowing down exponent near bifurcation points, etc., were all understood during this time.

## 6. Conclusions and Outlook

In this paper, we discussed the behavior of the Brusselator when driven by a periodic trigonometric force. This system was considered almost four decades ago, with the basic aim of understanding entrainment and the onset of chaos. Here, we consider a complementary situation, concerning the global organization of stability phases arising from *periodic motions of arbitrarily high periods*. Chaos is of collateral importance. After the coming-of-age of chaos, of great interest for us is to understand the partitioning and tiling of the control parameter space into series of stability phases and their accumulations. This description must include the classification of motions with all observable periodicities, the classification and study of the phases, and the investigation of their evolution as a function of as many control parameters as possible.

In recent year, the investigation of *autonomous* flows has revealed several unanticipated and wide-ranging organizations stability phases in the control parameter space of real-world practical applications.<sup>23–33</sup> Such findings uncover many enticing problems related to classical dissipative oscillators. For instance, nowadays there is an almost universal belief that Farey trees and entrainment would be inseparable partners in flows. In fact, the truth is that Farey trees are just a particular case of a more general and symmetric Stern-Brocot trees.<sup>42–44</sup> Both trees are generated by precisely the same mathematical rule and, therefore, are very easy to mix when not properly addressed. Thus, it is conceivable that the Stern-Brocot could play a more prominent role in the description of entrainment than hitherto appreciated, something that needs to be sorted out. Furthermore, it has also been found that these two trees might not be the only ones governing entrainment (e.g. an alternative possibility is discussed in connection with Fig. 7 in Ref. 24).

Traditionally, entrainment and quasiperiodicity have been studied almost invariably with the help of either non-autonomous flows or with maps slaved by “mod” functions. Both situations imply external forcing. In this context, the enticing open challenge is to study oscillators, governed by discrete-time equations or not, free from the shackles of the slaving introduced by extraneous frequencies. The reduction of higher-dimensional problems to the study of circle maps and rotation numbers may be convenient to demonstrate theorems and non-measurable properties but such reductions are not realistic or flexible enough to describe phenomena observed

in real life applications like e.g. the driven Brusselator, modulated CO<sub>2</sub> lasers, and other driven systems.

Reassuring to the continued effort to understand the global organization of periodic phases, of entrainment, and of quasiperiodicity is the fact that, with the steady improvement of computational resources, an insightful observation of Lorenz<sup>57</sup> remains as valid today as when stated originally in 1992: “*Now that computers have become ubiquitous, carefully conceived numerical experiments can enable us to explore a fascinating mathematical world that has not yet opened its doors to classical analytical procedures.*”

## Acknowledgments

The author thanks kind email exchanges and helpful advice received from Hao Bailin, Tohru Kai, Kunihiko Kaneko, Tohru Kohda, and Ichiro Tsuda. He also thanks Joana G. Freire and Marcia R. Gallas for help with computations and graphics. All bitmaps were computed at the CESUP-UFRGS clusters located in Porto Alegre, Brazil. The author was supported by CNPq, Brazil. This work was supported by the Deutsche Forschungsgemeinschaft through the Cluster of Excellence Engineering of Advanced Materials, and by the Max-Planck-Institut für Physik komplexer Systeme, Dresden, in the framework of the Advanced Study Group on Optical Rare Events.

## References

1. D. Aubin and A. D. Dalmedico, Writing the history of dynamical systems and chaos, *Longue durée and revolution, disciplines and cultures, Hist. Math.* **29** (2002) 273–339.
2. Y. Ueda, Randomly transitional phenomena in the system governed by Duffing’s equation, *J. Stat. Phys.* **20** (1978) 181–196.
3. Y. Ueda, *The Road to Chaos II*, 2nd edition (Aerial Press, Santa Cruz, 2001). Available free online: <http://repository.kulib.kyoto-u.ac.jp/dspace/handle/2433/71101?locale=en>.
4. R. J. Field, *Chaos in the Belousov-Zhabotinsky reaction*, Chapter in this volume (World Scientific, Singapore, 2015).
5. I. Prigogine and R. Balescu, Phénomènes cycliques dans la thermodynamique des processus irréversibles, *Bull. Cl. Sci. Acad. R. Belg.* **42** (1956) 256–265.
6. G. Nicolis and I. Prigogine, *Self-Organization in Equilibrium Systems* (Wiley, New York, 1977).
7. I. Prigogine and R. Lefever, Symmetry breaking instabilities in dissipative systems. II, *J. Chem. Phys.* **48** (1968) 1695–1700.
8. S. K. Scott, *Chemical Chaos* (Oxford University Press, Oxford, 1991).
9. R. Kremann, *Die periodischen Erscheinungen in der Chemie* (F. Enke Verlag, Stuttgart, 1913).
10. E. S. Hedges and J. E. Myers, *The Problem of Physico-Chemical Periodicity* (Arnold & Co., London, 1926).
11. A. Lotka, Zur Theorie der periodischen Reaktionen, *Z. Phys. Chem.* **72** (1910) 508–511.
12. J. Hirniak, Zur Frage der periodischen Reaktionen, *Z. Phys. Chem.* **75** (1910) 675–680.

13. A. Lotka, Contribution to the theory of periodic reactions, *J. Chem. Phys.* **14** (1910) 271–274.
14. A. Lotka, Ein fall von Autokatakinese mit oscillatorischem Verlauf, *Z. Phys. Chem.* **80** (1912) 159–164.
15. A. J. Lotka, Undamped oscillations derived from the law of mass action, *J. Am. Chem. Soc.* **42** (1920) 1595–1599.
16. J. J. Tyson, Some further studies of nonlinear oscillations in chemical systems, *J. Chem. Phys.* **58** (1973) 3919–3930.
17. I. R. Epstein and J. A. Pojman, *An Introduction to Nonlinear Chemical Dynamics* (Oxford University Press, New York, 1998).
18. R. Rosen, Book review of Self-Organization in Nonequilibrium System, *Int. J. Gener. Syst.* **4** (1978) 266–269.
19. H. Othmer, Book review of Self-Organization in Nonequilibrium System, *SIAM Review* **24** (1982) 483–485.
20. M. Han, P. Yu and N. Forms, *Melnikov Functions and Bifurcation of Limit Cycles* (Springer, London, 2012).
21. C. Christopher and C. Lin, *Limit Cycles of Differential Equations* (Birkhäuser, Basel, 2007).
22. V. A. Gaiko, *Global Bifurcation Theory and Hilbert's Sixteenth Problem* (Springer, New York, 2003).
23. J. G. Freire, R. Meucci, F. T. Arecchi and J. A. C. Gallas, Self-organization of pulsing and bursting in a CO<sub>2</sub> laser with opto-electronic feedback, *Chaos* **25** (2015) 097607.
24. M. R. Gallas and J. A. C. Gallas, Nested arithmetic progressions of oscillatory phases in Olsen's enzyme reaction model, *Chaos* **25** (2015) 064603.
25. M. J. B. Hauser and J. A. C. Gallas, Nonchaos-mediated mixed-mode oscillations in an enzyme reaction system, *J. Phys. Chem. Lett.* **5** (2014) 4187–4193.
26. A. Sack, J. G. Freire, E. Lindberg, T. Pöschel and J. A. C. Gallas, Discontinuous spirals of stable periodic oscillations, *Sci. Rep.* **3** (2013) 03350.
27. E. Pugliese, R. Meucci, S. Euzzor, J. G. Freire and J. A. C. Gallas, Complex dynamics of a dc glow discharge tube: Experimental modeling and stability diagrams, *Sci. Rep.* **5** (2015) 08447.
28. J. G. Freire, R. J. Field and J. A. C. Gallas, Relative abundance and structure of chaotic behavior: The nonpolynomial Belousov-Zhabotinsky reaction kinetics, *J. Chem. Phys.* **131** (2009) 044105.
29. L. Junges and J. A. C. Gallas, Intricate routes to chaos in the Mackey-Glass delayed feedback system, *Phys. Lett. A* **376** (2012) 2109–2116.
30. L. Junges and J. A. C. Gallas, Frequency and peak discontinuities observed in self-pulsations of a CO<sub>2</sub> laser with feedback, *Opt. Comm.* **285** (2012) 4500.
31. L. Junges and J. A. C. Gallas, Stability charts for continuous wide-range control of two mutually delay-coupled semiconductor lasers, *New J. Phys.* **17** (2015) 053038.
32. C. Bonatto, J. A. C. Gallas and Y. Ueda, Chaotic phase similarities and recurrences in a damped-driven Duffing oscillator, *Phys. Rev. E* **77** (2008) 026217.
33. M. A. Nascimento, J. A. C. Gallas and H. Varela, Self-organized distribution of periodicity and chaos in an electrochemical oscillator, *Phys. Chem. Chem. Phys.* **13** (2011) 441–446.
34. K. Tomita, T. Kai and F. Hikami, *Entrainment of a limit cycle by a periodic external excitation*, *Prog. Theor. Phys.* **57** (1977) 1159–1177.
35. K. Tomita and T. Kai, Stroboscopic phase portrait and strange attractors, *Phys. Lett. A* **66** (1978) 91–93.
36. K. Tomita and T. Kai, Chaotic behavior of deterministic orbits: The problem of turbulent phase, *Prog. Theor. Phys. Supplement* **64** (1978) 280–294.

37. K. Tomita and T. Kai, Chaotic response of a limit cycle, *J. Stat. Phys.* **21** (1979) 65–86.
38. T. Kai and K. Tomita, Stroboscopic phase portrait of a forced nonlinear oscillator, *Prog. Theor. Phys.* **61** (1979) 54–73.
39. K. Tomita, Chaotic response of nonlinear oscillators, *Phys. Rep.* **86** (1982) 113–167.
40. N. Minorsky, Nonlinear Oscillations, *Stroboscopic Method* (Chapter 16) (Van Nostrand, Princeton, 1962).
41. C. Knudsen, J. Sturis and J. S. Thomsen, Generic bifurcation of Arnold tongues in forced oscillators, *Phys. Rev. A* **44** (1991) 3503–3510.
42. J. G. Freire and J. A. C. Gallas, Stern-Brocot trees in the periodicity of mixed-mode oscillations, *Phys. Chem. Chem. Phys.* **13** (2011) 12191–12198.
43. J. G. Freire and J. A. C. Gallas, Stern-Brocot trees in cascades of mixed-mode oscillations and canards in the extended Bonhoeffer-van der Pol and the FitzHugh-Nagumo models of excitable systems, *Phys. Lett. A* **375** (2011) 1097–1103.
44. J. G. Freire, T. Pöschel and J. A. C. Gallas, Stern-Brocot trees in spiking and bursting of sigmoidal maps, *Europhys. Lett.* **100** (2012) 48002.
45. S. L. T. Souza, A. A. Lima, I. R. Caldas, R. O. Medrano-T and Z. O. Guimarães-Filho, Self-similarities of periodic structures for a discrete model of a two-gene system, *Phys. Lett. A* **376** (2012) 1290–1294.
46. M. R. Gallas, M. R. Gallas and J. A. C. Gallas, Distribution of chaos and periodic spikes in a three-cell population model of cancer, *Eur. Phys. J. Special Topics* **223** (2014) 2131–2144.
47. A. Hoff, D. T. da Silva, C. Manchein and H. A. Albuquerque, Bifurcation structures and transient chaos in a four-dimensional Chua model, *Phys. Lett. A* **378** (2014) 171–177.
48. B.-L. Hao and S.-Y. Zhang, Hierarchy of chaotic bands and periodicities embedded in them in a forced nonlinear oscillator, *Comm. Theor. Phys.* **1**(1) (1982) 111–115.
49. B.-L. Hao and S.-Y. Zhang, Subharmonic stroboscopy as a method to study period-doubling bifurcations, *Phys. Lett. A* **87** (1982) 267–270.
50. B.-L. Hao and S.-Y. Zhang, Hierarchy of chaotic bands, *J. Stat. Phys.* **28** (1982) 768–792.
51. B. L. Hao, G. R. Wang and S. Y. Zhang, U-sequences in the periodically forced Brusselator, *Commun. Theor. Phys.* **2** (1983) 1075–1080.
52. B. L. Hao, Symbolic dynamics and systematics of periodic windows, *Physica A* **140** (1986) 85–95.
53. B. L. Hao, *Elementary Symbolic Dynamics and Chaos in Dissipative Dynamical Systems* (World Scientific, Singapore, 1989).
54. B.-L. Hao and W.-M. Zheng, *Applied Symbolic Dynamics and Chaos* (World Scientific, Singapore, 1989).
55. B. Hao and W. Zheng, *Applied Symbolic Dynamics and Chaos*, 2nd revised edn. (Peking University Press, Beijing, 2014), ISBN 978-7-301-24756-3.
56. B. L. Hao, Bifurcation and chaos in the periodically forced Brusselator, in *Collected Papers Dedicated to Professor Kazuhisa Tomita on the Occasion of his Retirement from Kyoto University* (Kyoto University, 1987).
57. E. N. Lorenz, *The slow manifold — What is it?* *J. Atmos. Sci.* **49** (1992) 2449–2451.